Anti-inflammatory *ent*-Kaurane Diterpenoids from *Isodon serra*

Honghong Xing,[†] Lijun An,[†] Ziteng Song,[†] Shanshan Li,[†] Huimei Wang,[†] Chunyan Wang,[‡] Jie Zhang,[§] Muhetaer Tuerhong,[⊥] Munira Abudukeremu,[⊥] Dihua Li,[∥] Dongho Lee,[▽] Jing Xu,*[,†,O] Namrita Lall,[#] and Yuanqiang Guo*[,†]

[†]State Key Laboratory of Medicinal Chemical Biology, College of Pharmacy, and Tianjin Key Laboratory of Molecular Drug Research, Nankai University, Tianjin 300350, People's Republic of China

[‡]Tianjin Second People's Hospital, Tianjin 300192, People's Republic of China

[§]Key Laboratory for Green Processing of Chemical Engineering of Xinjiang Bingtuan, School of Chemistry and Chemical Engineering, Shihezi University, Shihezi 832003, People's Republic of China

[⊥]College of Chemistry and Environmental Sciences, Kashgar University, Kashgar 844000, People's Republic of China

[∥]Tianjin Institute of Acute Abdominal Diseases of Integrated Traditional Chinese and Western Medicine, Nankai Hospital Affiliated to Nankai University, Tianjin 300100, People's Republic of China

[▽]College of Life Sciences and Biotechnology, Korea University, Seoul 02841, Republic of Korea

[O]State Key Laboratory of Bioactive Substance and Function of Natural Medicines, Institute of Materia Medica, Chinese Academy of Medical Sciences and Peking Union Medical College, Beijing 100050, People's Republic of China

[#]Department of Plant and Soil Sciences, University of Pretoria, Pretoria 0002, South Africa

ABSTRACT: Ten new *ent*-kaurane diterpenoids, including two pairs of epimers **1**/**2** and **4**/**5** and a 6,7-*seco*-*ent*-kauranoid **10**, were obtained from the aerial parts of *Isodon serra*. The structures of the new compounds were confirmed by extensive spectroscopic methods and electronic circular dichroism (ECD) data analysis. An anti-inflammatory assay was applied to evaluate their nitric oxide (NO) inhibitory activities by using LPS-stimulated BV-2 cells. Compounds **1** and **9** exhibited notable NO production inhibition with IC_{50} values of 15.6 and 7.3 μM, respectively. Moreover, the interactions of some bioactive diterpenoids with inducible nitric oxide synthase (iNOS) were explored by employing molecular docking studies.

As one of the largest genera of the family Labiatae, *Isodon*, formally known as *Rabdosia* (Bl.) Hassk. and comprising approximately 150 species, is mainly distributed in tropical and subtropical Asia.[1] Over the last half a century, a series of phytochemical investigations of this genus have been conducted for its abundant diterpenoid constituents and their various biological activities.[2–4] As a result, over 1200 new diterpenoids have been isolated from *Isodon* plants,[2–21] including some *ent*-kauranoids with excellent antitumor and anti-inflammatory activities, such as oridonin,[22] eriocalyxin B,[23] and isoforretin A.[24]

Isodon serra (Maxim.) Kudo, a perennial plant, named, 'Xihuangcao' in China, is mainly distributed in Guangdong, Jiangxi, and Fujian provinces in China. As a Chinese folk medicine, *I. serra* has been popularly used to treat arthritis, enteritis, jaundice, hepatitis, and acute cholecystitis.[1] Some health-promoting foods and beverages derived from this plant are also popular in China. Previous phytochemical investigations on this species afforded abundant bioactive *ent*-kaurane diterpenoids,[25–30] involving enmein, spiro-lactone and C-20-nonoxygenated- and C-20-oxygenated-kauranoid types. With the aim of seeking structurally interesting and bioactive diterpenoids as lead compounds for inflammatory disease therapy, a phytochemical survey of the aerial parts of *I. serra* was conducted, which resulted in the isolation of 10 new *ent*-kauranoids, including two pairs of epimers **1**/**2** and **4**/**5** and a 6,7-*seco*-*ent*-kauranoid **10**. Some of these compounds showed promising NO inhibitory activities, which could potentially be useful for the treatment of inflammatory diseases. Here, the isolation, structure elucidation, and anti-inflammatory activities of these isolates as well as their interactions with the iNOS protein are described.

■ RESULTS AND DISCUSSION

Compound **1** was obtained as a white amorphous powder. Its molecular formula, $C_{24}H_{34}O_7$, was deduced from HRESIMS data analysis (*m/z* 457.2199 $[M + Na]^+$; calcd for $C_{24}H_{34}O_7Na$, 457.2202) and ^{13}C NMR data (Table 1), which indicated eight indices of hydrogen deficiency. The ^1H NMR spectroscopic data (Table 2) showed characteristic signals assignable to four methyl singlets (δ_H 0.80,

1.09, 2.01, and 2.18), two pairs of oxymethylene protons [δ_H 3.47 and 3.72 (each 1H, d, J = 11.5 Hz), and 3.84 and 4.04 (each 1H, d, J = 9.6 Hz)], and two oxymethine protons [δ_H 5.12 (1H, d, J = 7.0 Hz) and δ_H 5.16 (1H, s)]. The ^{13}C NMR and DEPT spectroscopic data (Table 1) exhibited 24 carbons, of which the signals at δ_C 173.6, 21.2, 170.4, and 21.6, along with two methyl singlets (δ_H 2.01 and 2.18), indicated the presence of two acetoxy groups. The remaining carbon signals comprised two methyls (δ_C 22.3 and 33.0), eight methylenes (δ_C 15.6, 18.5, 22.2, 24.8, 30.9, 41.1, 48.6, and 66.2), five methines (δ_C 41.0, 44.3, 54.5, 75.1, and 80.8), three quaternary carbons (δ_C 33.5, 35.8, and 52.7), an oxygenated tertiary carbon (δ_C 84.2), and an acetal carbon (δ_C 95.3) (Table 1). These spectroscopic features implied that compound **1** was a diterpenoid carrying two acetoxy groups.[31–35] Combining abundant *ent*-kaurane diterpenoids reported from *Isodon* species with these NMR data, particularly the acetal and oxymethylene carbons at δ_C 95.3 and 66.2, **1** was provisionally inferred to be a 7,20-epoxy-*ent*-kauranoid,[15,17,19,36–38] and 2D NMR experiments were thus performed to determine its full structure.

Analysis of 1D and 2D NMR data confirmed the 7,20-epoxy-*ent*-kauranoid skeletal structure, which comprised the 6/6/6 fused rings A, B, and C and the five-membered ring D consisting of C-8 and C-13–C-16 (Figure 1). Subsequently, the carbon and proton signals of the *ent*-kauranoid scaffold were assigned, of which the oxygenated or acetal carbons at δ_C 75.1, 95.3, 80.8, 84.2, and 66.2 were assigned to C-6, C-7, C-15, C-16, and C-20, respectively. There was one skeletal carbon remaining at δ_C 48.6, which was speculated to form a 16,17-epoxy moiety according to the distinctive chemical shift of C-17 (δ_C 48.6) and the total index of hydrogen deficiency, as well as the HMBC correlations shown in Figure 1. The HMBC correlations of H-6 and H-15 to the corresponding carbonyls of the acetoxy groups allowed for the two acetoxy moieties to be placed at C-6 and C-15 (Figure 1). In addition, a hydroxy moiety was assigned to C-7, an acetal carbon (δ_C 95.3). All of the NMR data analysis led to the 2D structure for **1**, as shown.

Analysis of its NOESY spectrum revealed the relative configuration of **1**. The cross-peaks observed for H_3-19/H-20a and H_3-18/H-5 but not for H-5/H-20a (20b) revealed rings that A and B were fused in a *trans*-configuration with a 7,20-epoxy moiety occupying the α-face of ring B (Figure 2). However,

the NOE correlations of H-9/H-5, H-15/H-5, and H-9/H-15 exhibited a *cis*-configuration for rings B and C with C-15 and H-9 occupying the *β*-face of ring C. In this molecular arrangement, ring A adopted a chair conformation, ring B a boat conformation due to the 7,20-epoxy group, and ring C also a boat conformation with the C-15−C-16 bridge link unit on the *β*-face (Figure 2). The C-6 acetoxy group was shown to be in a *β*-orientation based on the NOE correlation of H-6/H_3-19, which was supported by the $^3J_{5,6}$ coupling constant of 7.0 Hz. The C-15 acetoxy group was assigned an *α*-orientation from the NOESY interactions of H-15/H-5 and H-15/H-9. The configuration of C-16 was determined to be *rel*-16*R* according to the NOE correlations of H-17a (17b) with H-15, H-9, and H-12*β*.[39,40] To determine its absolute configuration, ECD calculations, a method applied extensively to define the absolute configuration of natural products,[41,42] were performed, and the calculated ECD curve of (5*R*,6*S*,7*S*,8*S*,9*S*,10*R*,13*R*,15*R*,16*R*)-**1** showed identical Cotton effects (CEs) to those in the experimental curve (Figure 3A). All of the abovementioned analyses defined the structure of isoserrin A (**1**) as (5*R*,6*S*,7*S*,8*S*,9*S*,10*R*,13*R*,15*R*,16*R*)-6*β*,15*α*-diacetoxy-7*α*,20:16*α*,17-diepoxy-7*β*-hydroxy-*ent*-kaurane.

The molecular formula of compound **2** (isoserrin B), $C_{24}H_{34}O_7$, inferred from the HRESIMS data, was shown to be identical to that of **1**. 1D NMR data analysis revealed that **2** had the same 7,20-epoxy-*ent*-kauranoid-type scaffold as **1** with two acetoxy groups, as concluded by 2D NMR data analysis. The HMBC correlations of H-6 and H-15 to the carbonyl resonances of the acetoxy groups (Figure 1) enabled the two acetoxy groups to be positioned at C-6 and C-15, respectively. Thus, the 2D structure of **2** was identical to that of **1**. However, their NMR data were somewhat different, suggesting a configurational difference between these two compounds. By comparing their ^{13}C NMR data (Table 1), upfield shifts of C-15 ($\Delta\delta$ −5.1) and C-16 ($\Delta\delta$ −10.2) in **2** were observed, which implied configurational changes of C-15 and C-16. NOESY data analysis of **2** (Figure 2) revealed the configuration as depicted in Figure 2, where the C-6 acetoxy group was in a *β*-orientation. The crucial NOE interactions of H-15/H-14*β*, H-17a (17b)/H-14*β*, H-15/H-17b, and H-17a/H-13 confirmed that the *rel*-15*R* and *rel*-16*R* configuration in **1** changed to *rel*-15*S* and *rel*-16*S* in **2**.[39,40] After defining the

relative configuration, the experimental and calculated ECD data depicted in Figure 3B showed close similarity, allowing for the structure of isoserrin B (**2**) to be defined as (5*R*,6*S*,7*S*,8*S*,9*S*,10*R*,13*R*,15*S*,16*S*)-6*β*,15*β*-diacetoxy-7*α*,20:16*β*,17-diepoxy-7*β*-hydroxy-*ent*-kaurane.

The ^{1}H and ^{13}C NMR spectra of compound **3** were similar to those of **2**, suggesting that these two compounds had the same 7,20-epoxy-*ent*-kauranoid-type scaffold with two acetoxy groups. The only difference was that one more oxygenated carbon signal (δ_C 75.9) occurred, replacing one of the aliphatic methylene carbons in **2**. The 1D and 2D NMR data of **2** showed that this additional signal was assigned to C-14 (δ_C 75.9). NOESY data revealed that the molecular conformation of **3** was identical to that of **2** (Figure 2). The C-14 hydroxy group was in a *β*-orientation instead of H-14*β* based on the NOESY correlations of H-20b/H-14 and H-14/H-11*α*. As in the case of **2**, by using ECD calculations and comparing the CEs in the calculated and experimental ECD curves (Figure 3C), the absolute configuration of **3** was assigned and the structure of isoserrin C (**3**) was defined as (5*R*,6*S*,7*S*,8*R*,9*S*,10*R*,13*R*,14*R*,15*S*,16*S*) -6*β*,15*β*-diacetoxy-7*α*,20:16*β*,17-diepoxy-7*β*,14*β*-dihydroxy-*ent*-kaurane.

Compound **4** gave a molecular formula of $C_{24}H_{36}O_8$, as analyzed by a sodium adduct ion at *m/z* 475.2307 $[M + Na]^+$ (calcd for $C_{24}H_{36}O_8Na$, 475.2308) in the (+)-HRESIMS analysis and the ^{13}C NMR data. The molecular formula indicated seven indices of hydrogen deficiency. Comparison of the ^{13}C NMR data of **4** with those of **1** revealed similarity, and the only difference was the change in the chemical shift of C-17 from δ_C 48.6 in **1** to δ_C 63.8 in **4**. This deshielding ($\Delta\delta$ +15.2) implied that the 16,17-epoxy ring in **1** was cleaved to form a 16,17-dihydroxy moiety in **4,** corresponding to the increase of 18 mass units and the absence of one index of hydrogen deficiency. The NOESY data showed that **4** possessed the same relative configuration as **1**, where the C-16 hydroxy group occupied an *α*-orientation based on the NOE correlations of H-17a (17b)/H-9. Using ECD calculations and comparing the CEs in the calculated and experimental curves (Figure 3D), the absolute configuration was assigned. Hence, the structure of isoserrin D (**4**) was defined as (5*R*,6*S*,7*S*,8*S*,9*S*,10*R*,13*R*,15*R*,16*R*)-6*β*,15*α*-diacetoxy-7*α*,20-epoxy-7*β*,16*α*,17-trihydroxy-*ent*-kaurane.

Compound **5** (isoserrin E) possessed the identical molecular formula as **4**, $C_{24}H_{36}O_8$, which was deduced from HRESIMS analysis as well as the ^{13}C NMR data. Furthermore, the 2D structure of **5** was also inferred to be the same as that of **4** by analyzing its 1D and 2D NMR data. However, there were some differences between their NMR data, suggesting that configurational changes were present. Upon comparison of the ^{13}C NMR data of compounds **4** and **5**, the shielding of C-15 ($\Delta\delta$ –6.1) and C-16 ($\Delta\delta$ –5.3) in **5** were evident and implied configurational changes of C-15 and C-16. This deduction was confirmed by NOESY data analysis, with H-15 and C-17 both being α-oriented in **5** (Figure 2). The identical CEs in the experimental and calculated ECD spectra (Figure 3D) permitted assignment of the structure of isoserrin E (**5**) as (5*R*,6*S*,7*S*,8*S*,9*S*,10*R*,13*R*,15*S*,16*S*)-6β,15β-diacetoxy-7α,20-epoxy-7β,16β,17-trihydroxy-*ent*-kaurane.

Compound **6** had a molecular formula of $C_{24}H_{34}O_8$ based on the HRESIMS (*m/z* 473.2148 [M + Na]$^+$; calcd for $C_{24}H_{34}O_8Na$, 473.2151) data analysis. From its ^1H and ^{13}C NMR spectra, two acetoxy moieties were detected. Differing from **1**–**5**, compound **6** had a 7,20-epoxy-*ent*-kaur-16-ene scaffold, which was subsequently verified by 2D NMR experiments. In addition, the skeletal proton and carbon signals were also assigned (Tables 1 and 3). The HMBC spectrum showed that the two acetoxy groups were attached at C-1 and C-15 using the long-range correlations of H-1 (δ_H 4.72) and H-15 (δ_H 6.05) to the corresponding carbonyls. In addition, three hydroxy groups were assigned at C-6, C-7, and C-14 based on the chemical shifts of C-6 (δ_C 73.1), C-7 (δ_C 98.3), and C-14 (δ_C 76.4), which was supported by the HRESIMS data. The NOESY experiment showed that the molecular conformation of **6** was similar to that of compound **3**, except for the C-16–C-17 terminal double bond replacing the 16,17-epoxy moiety in **3**. Furthermore, the acetoxy groups located at C-1 and C-15 and the hydroxy groups at C-6, C-7, and C-14 were assigned as being α-, β-, β-, β-, and β-oriented, respectively, from the NOESY interactions shown in Figure 2. As shown in Figure 3F, the calculated ECD spectrum of **6** displayed CEs analogous to the experimental ECD data, allowing the structure of isoserrin F (**6**) to be defined as (1*S*,5*R*,6*S*,7*S*,8*R*,9*S*,10*S*,13*S*,14*R*,15*R*)-1α,15β-diacetoxy-7α,20-epoxy-6β,7β,14β-trihydroxy-*ent*-kaur-16-ene.

The 1D NMR data indicated that compound **7** (isoserrin G) had the same 7,20-epoxy-*ent*-kaurane-16-ene skeleton with two acetoxy moieties. Comparison of its ^{13}C NMR data with those of **6** revealed that two more aliphatic methylene carbons were present, which replaced two oxygenated methine carbons in **6**. By analyzing the 2D NMR spectra, the 2D structure of **7** was established. The two additional aliphatic methylene signals at δ_C 31.3 and 26.1 were attributed to C-1 and C-14, which replaced the oxygenated methine at δ_C 76.2 (C-1) and 76.4 (C-14) in **6**. The relative configuration of **7** was similar to that of **6**, and the acetoxy groups at C-6 and C-15 were both *β*-oriented from the NOESY interactions displayed in Figure 2. The absolute configuration was again assigned by comparing the experimental and calculated ECD spectra (Figure 3G), that permitted definition of the structure of isoserrin G (**7**) as (5*R*,6*S*,7*S*,8*S*,9*S*,10*R*,13*R*,15*R*)-6*β*,15*β*-diacetoxy-7*α*,20-epoxy-7*β*-hydroxy-*ent*-kaur-16-ene.

Compound **8** (isoserrin H) was found to have the identical 7,20-epoxy-*ent*-kaur-16-ene scaffold as **7** according to the 1D and 2D NMR spectra. There were no acetoxy moieties present in **8**, and all the hydroxy groups were assigned to the oxygenated carbon signals based on the HRESIMS and NMR data. NOESY data analysis showed that the relative conformation of **8** remained the same as that of **7**, and the hydroxy groups attached to C-6, C-7, and C-15 were all *β*-oriented. The similar CEs displayed in the experimental and calculated ECD curves supported the structure of isoserrin H (**8**) as (5*R*,6*S*,7*S*,8*S*,9*S*,10*R*,13*R*,15*R*)-7*α*,20-epoxy-6*β*,7*β*,15*β*-trihydroxy-*ent*-kaur-16-ene.

The molecular formula of compound **9** (isoserrin I) was determined as $C_{24}H_{34}O_5$ by HRESIMS and ^{13}C NMR data analysis. Apart from the two acetoxy moieties disclosed in the 1D NMR spectra, 20 skeletal carbons detected in the ^{13}C NMR spectrum indicated that this compound was a diterpenoid. Comparing the 1D NMR data of **9** with those of compounds **1**–**8**, the notable difference in **9** was the presence of one more aliphatic methyl ($\delta_{C/H}$ 17.9/1.31) and a ketocarbonyl (δ_C 204.8), implying that the 7,20-epoxy ring was hydrolysed to form a methyl group by reduction of the hydroxymethyl group. This inference was corroborated by subsequent 2D NMR experiments. The long-range correlations of H-6 and H-15 to the carbonyls of the two acetoxy moieties (Figure 1) allowed for the two acetoxy groups to be placed at C-6 and C-15. The molecular arrangement of **9** is shown in Figure 2, with the

NOESY interactions observed for H-5/H_3-18, H-5/H-9, H-9/H-12β, H_3-19/H_3-20, H_3-19/H-6, and H_3-20/H-6, as well as other correlations. Correspondingly, the acetoxy groups attached at C-6 and C-15 were determined to both be β-oriented based on the NOE associations of H_3-19/H-6 and H-15/H-14β. The similar CEs shown in the experimental and calculated ECD curves supported the structure of isoserrin I (**9**) as (5*R*,6*S*,8*S*,9*S*,10*S*,13*R*,15*R*)-6β,15β-diacetoxy-*ent*-kaur-16-en-7-one.

Compound **10**, isolated as a white amorphous powder, gave a molecular formula of $C_{22}H_{32}O_6$, which was in agreement with the molecular ion at *m/z* 393.2271 $[M + H]^+$ (calcd for $C_{22}H_{33}O_6$, 393.2277) in the (+)-HRESIMS data analysis. This molecular formula required seven indices of hydrogen deficiency. Apart from an acetoxy moiety revealed by the signals (δ_C 170.4 and 21.5; δ_H 2.03), there were 20 skeletal carbons, comprising an ester carbonyl (δ_C 170.6), a ketocarbonyl (δ_C 216.3), and three oxygenated carbons (δ_C 76.3, 68.5, and 59.7). The remaining 15 aliphatic carbons were defined as three methyls, five methylenes, four methines, and three quaternary carbons using DEPT and HMQC experiments. The presence of a six-membered ring A was concluded via the HMBC cross-peaks of H_3-18/H_3-19 with C-3–C-5 and H-5 with C-1, C-3, C-4, and C-10, along with the ^{1}H–^{1}H COSY couplings of H-1/H_2-2/H_2-3 (Figure 1). Similarly, the six-membered ring C was deduced from the ^{1}H–^{1}H COSY correlations of H-9/H_2-11/H_2-12/H-13/H_2-14, as well as the HMBC correlations shown in Figure 1. In addition, the long-range correlations of H_3-17 to C-13, C-15, and C-16, together with the ^{1}H–^{1}H COSY cross-peaks of H_2-14/H-13/H-16/H_3-17, resulted in the establishment of the five-membered ring D, which carried a methyl (Me-17) group and shared C-8, C-13, and C-14 with ring C (Figure 1). There were three skeletal carbons left, including one ester carbonyl (δ_C 170.6) and two oxymethylenes (δ_C 68.4 and 59.7), of which the ester carbonyl and one of oxymethylenes were found to form a lactone ring composed of C-7–C-10 and C-20, which was confirmed by the HMBC correlations of H_2-20 to the carbonyl carbon at δ_C 170.6. The remaining oxymethylene was demonstrated to be attached at C-5 from the HMBC correlations depicted in Figure 1. Thus, a 15-oxo-6,7-*seco*-*ent*-kaur-7,20-olide scaffold was established. The HMBC correlations of H-1 (δ_H 4.78) to the carbonyl carbon at δ_C 170.4 allowed for this acetoxy group to be placed at C-1 (Figure 1). The NOESY correlations of H-5/H_3-18,

H-5/H-1, H-1/H-11α, H_3-19/H-20a, H-9/H-20b, H-9/H-6a (6b), H-12β/H_3-17, and H-9/H_3-17 showed a relative configuration, as depicted in Figure 2, in which C-16 was defined as *rel*-16*R*, and H-1, H-5, and C-20 were in the β-, β-, and α-orientations, respectively. The similar CEs shown in the experimental and calculated ECD curves supported the structure of isoserrin J (**10**) as (1*S*,5*R*,8*S*,9*S*,10*S*,13*R*,16*R*)-1α-acetoxy-6-hydroxy-15-oxo-6,7-*seco*-*ent*-kaur-7,20-olide.

In view of the widespread applications of *I. serra* to treat hepatitis and cholecystitis in traditional Chinese folk medicine, the new compounds were evaluated for their inhibitory effects on NO production in LPS-stimulated BV-2 cells.[43,44] The results (Table 4) showed that compounds **1** and **9** had significant inhibitory activities with IC_{50} values of 15.6 and 7.3 μM, respectively, while compounds **4**, **5**, and **7** exhibited moderate inhibitory activities. None of the compounds showed any cytotoxicity against BV-2 cells at their effective concentrations.

The inflammatory factor NO, which is catalyzed by the crucial enzyme iNOS of the inflammatory signaling pathway,[45] is the final product of the inflammatory response. Reduced NO production is usually the consequence of inhibited iNOS efficiency, and one useful method for reducing iNOS efficiency is to induce molecular binding between iNOS and other molecules through affinity interactions.[46] Thus, to understand the NO inhibitory mechanism, the possible affinity binding between iNOS and the bioactive compounds was predicted using molecular docking studies. As displayed in Figure 4, compounds **1**, **4**, **5**, **7**, and **9** with more inhibitory effects of NO production (IC_{50} < 50 μM) were selected, and the molecular docking results highlighted that these compounds had strong interactions with the iNOS protein. The binding residues and the logarithm of free binding energies are shown in Table 5.

Moreover, primary structure-activity relationship (SAR) studies of the new compounds were discussed based on the above biological assay. According to the NO inhibitory activities of **1**–**5**, the 16α,17-epoxy group, not the 16β,17-epoxy group, seemed to improve the activity (e.g., compound **1** vs **2**–**5**), and the cleavage of the 16 α,17-epoxy group resulted in a loss of potency (e.g., compounds **4** and **5** vs **1**). An α-oriented acetoxy group at C-1 in this class of diterpenoids seemed to decrease the

NO inhibitory potency (e.g., compound **6**). Compound **9** inhibited NO significantly, which indicated that 7-oxo would largely enhance the potency.

■ EXPERIMENTAL SECTION

General Experimental Procedures. Optical rotations and ECD spectra were recorded on an InsMark IP120 automatic polarimeter (InsMark Instrument Co., Ltd., Shanghai, People's Republic of China) and a JASCO J-715 CD spectrometer (JASCO Corporation, Tokyo, Japan), respectively. A Bruker Tensor 37 FT-IR spectrometer was used to record infrared (IR) spectra (KBr disks). All NMR experiments were conducted on a Bruker AV 400 instrument (Bruker, Switzerland, 100 MHz for ^{13}C and 400 MHz for ^{1}H NMR) with TMS as an internal reference at room temperature. ESIMS data were acquired on a Thermo Finnigan LCQ-Advantage mass spectrometer (Finnigan Co., Ltd., San Jose, CA, USA). HRESIMS data were recorded by an IonSpec 7.0 T FTICR MS (IonSpec Co. Ltd., Lake Forest, CA) or a VG ZAB-HS (VG Instruments, UK). HPLC separations were carried out on a CXTH system equipped with a Shodex RI-102 detector (Showa Denko Co., Ltd., Tokyo, Japan) and a YMC-pack ODS-AM (20 mm × 250 mm) column (YMC Co. Ltd., Kyoto, Japan). Medium-pressure liquid chromatography (MPLC) was performed with a P0100 pump, an ultraviolet (UV) detector (Huideyi Co., Beijing, People's Republic of China) and a column (40 mm × 400 mm) filled with octadecylsilane (ODS, 50 μm, YMC Co., Ltd.). Silica gel (200–300 mesh) used for column chromatography was obtained from Qingdao Haiyang Chemical Group Co., Ltd. (Qingdao, People's Republic of China). Chemical reagents (analytical grade) and biological reagents were provided by Tianjin Chemical Reagent Co. (Tianjin, People's Republic of China) and Sigma Co., respectively. The BV-2 cell line was obtained from Shanghai Institutes for Biological Sciences, Chinese Academy of Sciences (Shanghai, People's Republic of China).

Plant Material. The aerial parts of *I. serra* were purchased from Anguo Herbal Medicine Market, Hebei Province, People's Republic of China, in April 2018 and identified by Lipei Yang (Anguo Jufu Pharmaceutical Co., Ltd., Anguo, People's Republic of China). A voucher specimen (No. 20180401) was stored at the laboratory of Natural Medicinal Chemistry, Nankai University.

Extraction and Isolation. The air-dried aerial parts of *I. serra* (12.0 kg) were extracted with MeOH (3 × 60 L) under reflux, and the resulting solution was concentrated *in vacuo* to yield a residue (1.3 kg). This residue was dissolved in H_2O and partitioned with petroleum ether and EtOAc, successively. The petroleum ether-soluble portion (267.2 g) was subjected to silica gel CC (silica gel, 200–300 mesh, 1200 g; column, 10 cm × 50 cm) with petroleum ether–acetone (100: 0, 100: 2, 100: 4, 100: 6, 100: 9, 100: 12, 100: 17, 100: 25, and 100: 32; 21 L for each gradient elution) as the eluent to yield nine fractions, A–I, based on TLC analysis. Fraction H (28.5 g) was further separated by MPLC (octadecylsilane, ODS) and eluted with a stepwise gradient of 62–91% MeOH in H_2O to yield seven subfractions, H1–H7. Fraction H4 was purified using preparative HPLC (YMC-pack ODS-AM column, 20 mm × 250 mm) to afford compound **1** (t_R 38 min, 6.1 mg) with the eluent of 80% MeOH in H_2O. Similarly, compounds **6** (t_R 36 min, 2.9 mg) and **10** (t_R 29 min, 9.6 mg) were isolated from fractions H3 (71% MeOH in H_2O) and H1 (62% MeOH in H_2O), respectively, by using the same HPLC system. Fraction G (20.0 g) was subjected to the same MPLC protocol using the eluent of 62–91% MeOH in H_2O to provide eight subfractions, G1–G8. The subsequent purification of subfraction G5 was conducted with the same HPLC protocol (79% MeOH in H_2O) to produce compounds **2** (t_R 29 min, 11.4 mg) and **8** (t_R 33 min, 8.8 mg). Isolation of fraction I (58.5 g, 62–91% MeOH in H_2O) yielded seven subfractions, I1–I7, using the above MPLC system, and the purification of I3 (72% MeOH in H_2O) yielded compounds **3** (t_R 34 min, 14.2 mg), **4** (t_R 39 min, 16.7 mg), and **5** (t_R 35 min, 7.1 mg) with the same HPLC system. Likewise, fraction D (28.0 g) was divided into eight subfractions, D1–D8, by MPLC (67–94% MeOH in H_2O), and compound **7** (t_R 33 min, 9.5 mg) was obtained by preparative HPLC (86% MeOH in H_2O). With the same procedure as used for fraction D, eight subfractions, C1–C8, were obtained from fraction C (13.0 g), and compound **9** (t_R 27 min, 10.5 mg) was subsequently obtained through the purification of subfraction C5 by the same HPLC method (90% MeOH in H_2O).

*Isoserrin A (**1**):* white amorphous powder; $[\alpha]_D^{17}$ –47 (*c* 0.3, CH_2Cl_2); ECD (CH_3CN) 216 ($\Delta\varepsilon$ +2.22) nm; IR (KBr) ν_{max} 3482, 2953, 2926, 1734, 1458, 1375, 1248, 1050, 735 cm^{-1}; ^{13}C NMR (100

MHz, $CDCl_3$) and ^1H NMR (400 MHz, $CDCl_3$) data, see Tables 1 and 2; ESIMS *m/z* 457 $[M + Na]^+$; HRESIMS *m/z* 457.2199 $[M + Na]^+$, calcd for $C_{24}H_{34}O_7Na$, 457.2202.

*Isoserrin B (**2**):* colorless oil; $[\alpha]_D^{17}$ −74 (*c* 0.5, CH_2Cl_2); ECD (CH_3CN) 215 ($\Delta\varepsilon$ +2.27) nm; IR (KBr) ν_{max} 3367, 2950, 2927, 1738, 1375, 1249, 1054, 736 cm^{-1}; ^{13}C NMR (100 MHz, $CDCl_3$) and ^1H NMR (400 MHz, $CDCl_3$) data, see Tables 1 and 2; ESIMS *m/z* 457 $[M + Na]^+$; HRESIMS *m/z* 457.2199 $[M + Na]^+$, calcd for $C_{24}H_{34}O_7Na$, 457.2202.

*Isoserrin C (**3**):* colorless oil (MeOH); $[\alpha]_D^{17}$ −73 (*c* 0.1, MeOH); ECD (CH_3CN) 213 ($\Delta\varepsilon$ +1.84) nm; IR (KBr) ν_{max} 3310, 2925, 2853, 1736, 1458, 1374, 1248, 1048 cm^{-1}; ^{13}C NMR (100 MHz, $CDCl_3$) and ^1H NMR (400 MHz, $CDCl_3$) data, see Tables 1 and 2; ESIMS *m/z* 473 $[M + Na]^+$; HRESIMS *m/z* 473.2149 $[M + Na]^+$, calcd for $C_{24}H_{34}O_8Na$, 473.2151.

*Isoserrin D (**4**):* colorless oil; $[\alpha]_D^{17}$ −10 (*c* 0.3, MeOH); ECD (CH_3CN) 215 ($\Delta\varepsilon$ +1.26) nm; IR (KBr) ν_{max} 3355, 2926, 2854, 1734, 1458, 1375, 1253, 1046 cm^{-1}; ^{13}C NMR (100 MHz, $CDCl_3$) and ^1H NMR (400 MHz, $CDCl_3$) data, see Tables 1 and 2; ESIMS *m/z* 475 $[M + Na]^+$; HRESIMS *m/z* 475.2307 $[M + Na]^+$, calcd for $C_{24}H_{36}O_8Na$, 475.2308.

*Isoserrin E (**5**):* colorless oil; $[\alpha]_D^{17}$ −27 (*c* 0.2, MeOH); ECD (CH_3CN) 211 ($\Delta\varepsilon$ +0.63) nm; IR (KBr) ν_{max} 3311, 2926, 2854, 1734, 1458, 1375, 1251, 1051 cm^{-1}; ^{13}C NMR (100 MHz, $CDCl_3$) and ^1H NMR (400 MHz, $CDCl_3$) data, see Tables 1 and 2; ESIMS *m/z* 475 $[M + Na]^+$; HRESIMS *m/z* 475.2308 $[M + Na]^+$, calcd for $C_{24}H_{36}O_8Na$, 475.2308.

*Isoserrin F (**6**):* colorless oil; $[\alpha]_D^{17}$ −41 (*c* 0.4, CH_2Cl_2); ECD (CH_3CN) 210 ($\Delta\varepsilon$ +0.60) nm; IR (KBr) ν_{max} 3325, 2953, 2925, 2854, 1737, 1458, 1374, 1242, 1042 cm^{-1}; ^{13}C NMR (100 MHz, $CDCl_3$) and ^1H NMR (400 MHz, $CDCl_3$) data, see Tables 1 and 3; ESIMS *m/z* 473 $[M + Na]^+$; HRESIMS *m/z* 473.2148 $[M + Na]^+$, calcd for $C_{24}H_{34}O_8Na$, 473.2151.

*Isoserrin G (**7**):* colorless prisms (MeOH); $[\alpha]_D^{17}$ −88 (*c* 0.4, CH_2Cl_2); ECD (CH_3CN) 217 ($\Delta\varepsilon$ +2.71) nm; IR (KBr) ν_{max} 3356, 2927, 2868, 1736, 1497, 1375, 1252, 1056, 987, 874, 737 cm^{-1}; ^{13}C NMR (100 MHz, $CDCl_3$) and ^1H NMR (400 MHz, $CDCl_3$) data, see Tables 1 and 3; ESIMS *m/z* 441 $[M + Na]^+$; HRESIMS *m/z* 441.2251 $[M + Na]^+$, calcd for $C_{24}H_{34}O_6Na$, 441.2253.

*Isoserrin H (**8**):* colorless oil (MeOH); $[\alpha]_D^{17}$ −38 (*c* 0.2, MeOH); ECD (CH_3CN) 207 (Δε +2.80) nm; IR (KBr) ν_{max} 3337, 2924, 2853, 1735, 1718, 1457, 1374, 1250, 1056, 944 cm^{-1}; ^{13}C NMR (100 MHz, $CDCl_3$) and ^1H NMR (400 MHz, $CDCl_3$) data, see Tables 1 and 3; ESIMS *m/z* 357 $[M + Na]^+$; HRESIMS *m/z* 357.2040 $[M + Na]^+$, calcd for $C_{20}H_{30}O_4Na$, 357.2042.

*Isoserrin I (**9**):* colorless oil; $[\alpha]_D^{17}$ −56 (*c* 0.1, CH_2Cl_2); ECD (CH_3CN) 219 (Δε +1.12), 286 (Δε +1.49) nm; IR (KBr) ν_{max} 3446, 2955, 2924, 2852, 1748, 1718, 1458, 1376, 1234, 1089, 976, 801 cm^{-1}; ^{13}C NMR (100 MHz, $CDCl_3$) and ^1H NMR (400 MHz, $CDCl_3$) data, see Tables 1 and 3; ESIMS *m/z* 425 $[M + Na]^+$; HRESIMS *m/z* 425.2302 $[M + Na]^+$, calcd for $C_{24}H_{34}O_5Na$, 425.2304.

*Isoserrin J (**10**):* white amorphous powder; $[\alpha]_D^{17}$ −217 (*c* 0.6, CH_2Cl_2); ECD (CH_3CN) 200 (Δε −5.11), 310 (Δε −0.41) nm; IR (KBr) ν_{max} 3462, 2955, 2926, 1739, 1718, 1458, 1396, 1260, 1119, 1044 cm^{-1}; ^{13}C NMR (100 MHz, $CDCl_3$) and ^1H NMR (400 MHz, $CDCl_3$) data, see Tables 1 and 3; ESIMS *m/z* 393 $[M + H]^+$; HRESIMS *m/z* 393.2271 $[M + H]^+$, calcd for $C_{22}H_{33}O_6$, 393.2277.

ECD Calculations. The relative configuration of each compound was deduced from the NOESY spectrum and Chem3D modeling. MOE software was applied to give systematic conformational searches of each compound, and appropriate conformers were selected for geometry optimizations. The optimizations and re-optimizations at the B3LYP/6–31 + G(d,p) level were carried out with the Gaussian 09 package,[47] and TDDFT ECD calculations for the optimized conformers were performed at the CAM-B3LYP/SVP level with a CPCM solvent model in MeCN. The calculated ECD spectra of different conformers were simulated with a half bandwidth of ~ 0.4 eV, and the ECD curves were extracted with SpecDis 1.62 software.[48] All the ECD curves of each compound were weighted by Boltzmann distribution after UV correction.

Assay for NO Inhibitory Activities. The NO inhibitory activities were measured as described previously.[43,44]

Molecular Docking Studies. Molecular docking simulations were performed by the software AutoDock Vina along with AutoDock Tools (ADT 1.5.6) using the hybrid Lamarckian Genetic Algorithm (LGA). The 3D crystal structure of iNOS (PDB code, 3E6T; resolution, 2.5 Å) was obtained

from the RCSB Protein Data Bank.[46] According to NOESY spectra and Chem3D modeling, the standard 3D structures (PDB format) of selected compounds were established by chem3D Pro 14.0 software. A cubic grid box 20 Å in size (x, y, z) with a spacing of 1.000 Å and grid maps was built. Other parameters used were based on default settings of AutoDock Vina. The results differing by less than 2.0 Å in positional root-mean-square deviation (RMSD) were clustered together, and the results of the most favorable free binding energy (FBE) were chosen as the resultant complex structures.

■ ASSOCIATED CONTENT

● Supporting Information

The Supporting Information is available free of charge on the ACS Publications website at DOI:

The NMR, IR, and HRESIMS spectra of compounds **1**–**10**.

■ AUTHOR INFORMATION

Corresponding Authors

*Tel/Fax (J. Xu): 86-22-23506290. E-mail: xujing611@nankai.edu.cn.

*Tel/Fax (Y. Guo): 86-22-23507760. E-mail: victgyq@nankai.edu.cn.

ORCID

Jing Xu: 0000-0003-0847-4510

Yuanqiang Guo: 0000-0002-5297-0223

Notes

The authors declare no competing financial interest.

■ ACKNOWLEDGMENTS

This research was supported financially by the National Key Research and Development Program of China (No. 2018YFA0507204), the National Natural Science Foundation of China (Nos. U1703107, U1801288, and 21665013), the Natural Science Foundation of Tianjin, China (No. 19JCYBJC28100), Hundred Young Academic Leaders Program of Nankai University, State Key Laboratory of Bioactive

Substance and Function of Natural Medicines (Institute of Materia Medica, Chinese Academy of Medical Sciences and Peking Union Medical College, No. GTZK201902), and the open project of Key Laboratory of Xinjiang Uygur Autonomous Region (Nos. 2015KL030 and 2017D04019).

REFERENCES

(1) Editorial Committee of the Flora of China, Chinese Academy of Sciences. *Flora of China*; Vol. *66*; Science Press: Beijing, 1977; pp. 416–434.

(2) Sun, H. D.; Huang, S. X.; Han, Q. B. *Nat. Prod. Rep*. **2006**, *23*, 673−698.

(3) Liu, M.; Wang, W. G.; Sun, H. D.; Pu, J. X. *Nat. Prod. Rep*. **2017**, *34*, 1090−1140.

(4) Cheng, W. Y.; Huang, C. H.; Ma, W. F.; Tian, X.; Zhang, X. J. *Mini-Rev. Med. Chem.* **2019**, *19*, 114−124.

(5) Wen, C. M.; Chen, S.; Yuan, F.; Liu, X. M.; Song, F. J.; Mei, Z. N.; Yang, X. F.; Yang, G. S. *RSC Adv.* **2019**, *9*, 40628–40635.

(6) Liu, Y. L; Zhang, L. X.; Wu, H.; Chen, S. Q.; Li, J.; Dai, L. P.; Wang, Z. M. *Molecules* **2019**, *24*, 2736−2745.

(7) Chen, W. F.; Wong, L. L.; Zhang, X.; Zhou, F. X.; Xia, F.; Tang, L. P.; Li, X. *Chem. Biodivers.* **2019**, *16*, e1900206−e1900212.

(8) Gou, L. L.; Hu, K.; Yang, Q.; Li, X. N.; Sun, H. D.; Xiang, C. L.; Puno, P. T. *Tetrahedron* **2019**, *75*, 2797−2806.

(9) Hu, J.; Li, X. R.; Tian, W. F.; Lu, Y. T.; Xu, Y. H.; Wang, F.; Qin, W. Y.; Ma, X. L.; Puno, P. T.; Xiong, W. Y. *Molecules* **2019**, *24*, 158−173.

(10) Chen, L.; Yang, Q.; Hu, K.; Li, X. N.; Sun, H. D.; Puno, P. T. *Fitoterapia* **2019**, *134*, 158−164.

(11) Xiang, P.; Xiao, C. J.; Xu, W.; Shan, H.; Qiu, L.; Li, Y.; Dong, X.; Jiang, B. *J. Asian Nat. Prod. Res.* **2019**, *21*, 1177−1183.

(12) Yang, Q.; Hu, K.; Yan, B. C.; Liu, M.; Li, X. N.; Sun, H. D.; Puno, P. T. *Org. Chem. Front.* **2019**, *6*, 45−53.

(13) Hu, Z. X.; Xu, H. C.; Hu, K.; Liu, M.; Li, X. N.; Li, X. R.; Du, X.; Zhang, Y. H.; Puno, P. T.; Sun, H. D. *Org. Chem. Front.* **2018**, *5*, 2379−2389.

(14) Li, X. R.; Fu, Q.; Zhou, M.; Hu, K.; Du, X.; Li, X. N.; Sun, H. D.; Yue, J. B.; Zhang, H. B.; Puno, P. T. *J. Asian Nat. Prod. Res.* **2019**, *21*, 977−984.

(15) Hu, Z. X.; Liu, M.; Wang, W. G.; Li, X. N.; Hu, K.; Li, X. R.; Du, X.; Zhang, Y. H.; Puno P. T.; Sun, H. D. *J. Nat. Prod.* **2018**, *81*, 106−116.

(16) Luo, G. Y.; Deng, R.; Zhang, J. J.; Ye, J. H.; Pan, L. T. *J. Asian Nat. Prod. Res.* **2018**, *20*, 227−233.

(17) Zhang, Y. Y.; Jiang, H. Y.; Liu, M.; Hu, K.; Wang, W, G; Du, X.; Li, X. N.; Pu, J. X.; Sun, H. D. *Phytochemistry* **2017**, *143*, 199−207.

(18) Matsumoto, T.; Nakamura, S.; Kojima, N.; Hasei, T.; Yamashita, M.; Watanabe, T.; Matsuda, H. *Tetrahedron Lett.* **2017**, *58*, 3574–3578.

(19) Jiang, H. Y.; Wang, W. G.; Tang, G. W.; Liu, M.; Li, X. R.; Hu, K.; Du, X.; Li, X. N.; Zhang, H. B.; Pu, J. X.; Sun, H. D. *J. Nat. Prod.* **2017**, *80*, 2026−2036.

(20) Yang, J.; Wang, W. G.; Wu, H. Y.; Liu, M.; Jiang, H. Y.; Du, X.; Li, Y.; Pu, J. X.; Sun, H. D. *Tetrahedron Lett*. **2017**, *58*, 349−351.

(21) Yang, J.; Wang, W. G.; Wu, H. Y.; Du, X.; Li, X. N.; Li, Y.; Pu, J. X.; Sun, H. D. *J. Nat. Prod.* **2016**, *79*, 132−140.

(22) Li, D. H.; Han, T.; Liao, J.; Hu, X.; Xu, S. T.; Tian, K. T.; Gu, X. K.; Cheng, K. G.; Li, Z. L.; Hua, H. M. *Int. J. Mol. Sci.* **2016**, *17*, 1395−1412.

(23) Sun, H. D.; Lin, Z. W.; Niu, F. D.; Shen, P. Q.; Pan, L. T.; Lin, L. Z.; Cordell, G. A. *Phytochemistry* **1995**, *38*, 1451−1455.

(24) Sun, X.Y.; Wang, W. G; Chen, J.; Cai, X. T.; Yang, J.; Yang, Y.; Yan, H. J.; Cheng, X. L.; Ye, J.; Lu, W. G. *Cancer Res.* **2017**, *77*, 926−936.

(25) Wan, J.; Jiang, H. Y.; Tang, J. W.; Li, X. R.; Du, X.; Li, Y.; Sun, H. D.; Pu, J. X. *Molecules* **2017**, *22*, 309−318.

(26) Wan, J.; Liu, M.; Jiang, H. Y.; Yang, J.; Du, X.; Li, X. N.; Wang, W. G.; Li, Y.; Pu, J. X.; Sun, H. D. *Phytochemistry* **2016**, *130*, 244−251.

(27) Wang, W. Q.; Xuan, L. J. *Phytochemistry* **2016**, *122*, 119−125.

(28) Yan, F. L.; Xie, R. J.; Yin, Y. Y.; Zhang, Q. *J. Chem. Res.* **2012**, *36*, 523−524.

(29) Yan, F. L.; Zhang, L. B.; Zhang, J. X.; Sun, H. D. *Chinese Chem. Lett.* **2007**, *18*, 1383−1385.

(30) Zhao, A. H.; Zhang, Y.; Xu, Z. H.; Liu, J. W.; Jia, W. *Helv. Chim. Acta* **2004**, *87*, 3160−3166.

(31) Li, J.; Pan, L.; Fletcher, J. N.; Lv, W.; Deng, Y.; Vincent, M. A.; Slack, J. P.; McCluskey, T. S.; Jia, Z.; Cushman, M.; Kinghorn, A. D. *J. Nat. Prod.* **2014**, *77*, 1739−1743.

(32) Pan, L.; Terrazas, C.; Lezama-Davila, C. M.; Rege, N.; Gallucci, J. C.; Satoskar, A. R.; Kinghorn, A. D. *Org. Lett.* **2012**, *14*, 2118–2121.

(33) Fullas, F.; Hussain, R. A.; Chai, H. B.; Pezzuto, J. M.; Soejarto, D. D.; Kinghorn, A. D. *J. Nat. Prod.* **1994**, *57*, 801–807.

(34) Bautista, E.; Toscano, R. A.; Ortega, A. *J. Nat. Prod.* **2014**, *77*, 1088–1092.

(35) Bautista, E.; Toscano, A.; Calzada, F.; Díaz, E.; Yépez-Mulia, L.; Ortega, A. *J. Nat. Prod.* **2013**, *76*, 1970–1975.

(36) Hong, S. S.; Lee, S. A; Lee, C.; Han, X. H.; Choe, S.; Kim, N.; Lee, D.; Lee, C. K.; Kim, Y.; Hong, J. T.; Lee, M. K; Hwang, B. Y. *J. Nat. Prod.* **2011**, *74*, 2382−2387.

(37) Hong, S. S; Lee, S. A.; Han, X. H.; Hwang, J. S.; Lee, C.; Lee, D; Hong, J. T; Kim, Y.; Lee, H.; Hwang, B. Y. *J. Nat. Prod.* **2008**, *71*, 1055−1058.

(38) Hong, S. S.; Lee, S. A.; Han, X. H.; Jin, H. Z.; Lee, J. H.; Lee, D.; Lee, J. J.; Hong, J. T.; Kim, Y.; Ro, J. S.; Hwang, B. Y. *J. Nat. Prod.* **2007**, *70*, 632−636.

(39) Chen, S. N.; Yue, J. M.; Chen, S. Y.; Lin, Z. W.; Qin, G. W.; Sun, H. D.; Chen, Y. Z. *J. Nat. Prod.* **1999**, *62*, 782−784.

(40) Wang, Z. Q.; Wang, X. R.; Dong, J. G.; Wang, X. W. *Acta Bot. Sin.* **1986**, *28*, 185–191.

(41) Li, X. C.; Ferreira, D.; Ding, Y. *Curr. Org. Chem.* **2010**, *14*, 1678−1697.

(42) Xu. J.; Kang, J.; Sun, X. C.; Cao, X. R; Rena, K.; Lee, D.; Ren, Q. H.; Li, S.; Ohizumi, Y.; Guo, Y. Q. *J. Nat. Prod*. **2016**, *79*, 170−179.

(43) Liang, Y.; An, L. J.; Shi, Z. Y.; Zhang, X. K.; Xie, C. F.; Tuerhong, M.; Song, Z. H.; Ohizumi, Y.; Lee, D.; Shuai, L.; Xu, J.; Guo, Y. Q. *J. Nat. Prod*. **2019**, *82*, 1634−1644.

(44) Wang, P. X.; Xie, C. F.; An, L. J.; Yang, X. Y.; Xi, Y. R.; Yuan, S.; Zhang, C. Y.; Tuerhong, M.; Jin, D. Q.; Lee, D.; Zhang, J.; Ohizumi, Y.; Xu, J.; Guo, Y. Q. *J. Nat. Prod*. **2019**, *82*, 183−193.

(45) Lee S. R.; Lee, S.; Moon, E.; Park, H. J.; Park, H. B.; Kim, K. H. *Bioorg. Chem.* **2017**, *70*, 94–99.

(46) Garcin, E. D.; Arvai, A. S.; Rosenfeld, R. J.; Kroeger, M. D.; Crane, B. R.; Andersson, G.; Andrews, G.; Hamley, P. J.; Mallinder, P. R.; Nicholls, D. J.; St-Gallay, S. A.; Tinker, A. C.; Gensmantel, N. P.; Mete, A.; Cheshire, D.

R.; Connolly, S.; Stuehr, D. J.; Aberg, A.; Wallace, A. V.; Tainer, J. A.; Getzoff, E. D. *Nat. Chem. Biol.* **2008**, *4*, 700−707.

(47) Frisch, M. J.; Trucks, G. W.; Schlegel, H. B.; Scuseria, G. E.; Robb, M. A.; Cheeseman, J. R.; Scalmani, G.; Barone, V.; Mennucci, B.; Petersson, G. A.; Nakatsuji, H.; Caricato, M.; Li, X.; Hratchian, H.P.; Izmaylov, A. F.; Bloino, J.; Zheng, G.; Sonnenberg, J. L.; Hada, M.; Ehara, M.; Toyota, K.; Fukuda, R.; Hasegawa, J.; Ishida, M.; Nakajima, T.; Honda, Y.; Kitao, O.; Nakai, H.; Vreven, T.; Montgomery Jr., J.A.; Peralta, J. E.; Ogliaro, F.;Bearpark, M.; Heyd, J.J.; Brothers, E.; Kudin, K.N.; Staroverov, V. N.; Kobayashi, R.; Normand, J.; Raghavachari, K.; Rendell, A.; Burant, J. C.; Iyengar, S. S.; Tomasi, J.; Cossi, M.; Rega, N.; Millam, J. M.; Klene, M.; Knox, J. E.; Cross, J. B.; Bakken, V.; Adamo, C.; Jaramillo, J.; Gomperts, R.; Stratmann, R. E.; Yazyev, O.; Austin, A. J.; Cammi, R.; Pomelli, C.; Ochterski, J. W.; Martin, R. L.; Morokuma, K.; Zakrzewski, V. G.; Voth, G. A.; Salvador, P.; Dannenberg, J. J.; Dapprich, S.; Daniels, A. D.; Farkas, O.; Foresman, J. B.; Ortiz, J. V.; Cioslowski, J.; Fox, D. J. Gaussian 09, Revision B.01, Gaussian, Inc., Wallingford, CT, 2010.

(48) Bruhn, T.; Schaumloffel, A.; Hemberger, Y.; Bringmann, G. SpecDis, version 1.62; University of Wuerzburg: Wuerzburg, Germany, 2014.

Table Captions

Table 1. ^{13}C NMR Data for Compounds **1**–**10**.

Table 2. ^{1}H NMR Data for Compounds **1**–**5**.

Table 3. ^{1}H NMR Data for Compounds **6**–**10**.

Table 4. IC_{50} Values of Compounds **1**–**10** Inhibiting NO Production in BV-2 Cells.

Table 5. Logarithms of Free Binding Energies (FBE, kcal/mol) of NO Inhibitors to the Active Cavities of iNOS (PDB code: 3E6T) and Targeting Residues of the Binding Site Located on the Mobile Flap.

Table 1. **^{13}C NMR Data for Compounds 1–10** ($CDCl_3$, 100 MHz, δ in ppm)

position	**1**	**2**	**3**	**4**	**5**	**6**	**7**	**8**	**9**	**10**
1	30.9	30.8	31.2	30.9	31.0	76.2	31.3	30.6	40.5	76.3
2	18.5	18.5	18.5	18.5	18.5	25.2	18.6	18.7	18.1	23.9
3	41.1	41.0	41.2	41.1	41.1	38.3	41.2	41.1	43.3	39.5
4	33.5	33.5	33.5	33.5	33.5	33.2	33.4	33.6	34.0	33.7
5	54.5	54.4	54.3	54.4	54.1	55.1	53.4	57.2	55.0	52.8
6	75.1	75.2	73.1	75.2	75.5	73.1	75.6	73.6	75.5	59.7
7	95.3	95.4	97.4	95.3	95.3	98.3	95.6	96.8	204.8	170.6
8	52.7	51.7	53.3	52.4	51.6	52.1	50.4	51.1	58.2	58.3
9	44.3	44.4	46.2	44.3	44.4	46.4	44.5	41.9	47.3	41.4
10	35.8	35.9	35.6	35.9	35.9	39.1	36.0	35.9	39.8	43.2
11	15.6	15.6	15.3	15.6	14.8	16.4	15.2	15.0	17.1	16.9
12	22.2	25.6	25.8	21.5	19.0	31.5	31.6	32.2	32.7	19.3
13	41.0	36.4	44.2	40.1	37.0	45.0	36.0	36.1	39.5	31.9
14	24.8	26.4	75.9	25.3	24.2	76.4	26.1	25.5	34.0	30.8
15	80.8	75.7	74.9	81.1	75.0	72.4	74.5	73.8	75.7	216.3
16	84.2	74.0	73.8	84.7	79.4	156.1	158.2	160.3	151.8	48.2
17	48.6	48.6	47.3	63.8	70.3	111.8	108.9	107.8	108.0	11.5
18	33.0	32.9	32.7	32.9	33.0	32.7	33.3	33.0	35.6	33.3
19	22.3	22.3	22.2	22.3	22.4	22.0	22.6	22.1	21.7	23.6
20	66.2	66.3	66.4	66.3	66.5	63.3	66.6	66.2	17.9	68.5
AcO-1						170.2				170.4
						21.6				21.5
AcO-6	173.6	173.6	171.5	173.4	173.5		173.9		170.0	
	21.2	21.1	21.1	21.1	21.0		21.2		21.1	
AcO-15	170.4	169.9	169.8	171.3	172.2	171.6	170.7		170.0	
	21.6	21.6	21.6	21.5	21.7	21.8	22.0		21.2	

Table 2. **^{1}H NMR Data for Compounds 1–5** ($CDCl_3$, 400 MHz, δ in ppm, J in Hz)

position	**1**	**2**	**3**	**4**	**5**
1α	1.46, m	1.49, m	1.42, m	1.44, m	1.47, m
1β	1.10, m	1.14, m	1.06, m	1.10, m	1.18, m
2α	1.48, m	1.49, m	1.48, m	1.49, m	1.47, m
2β	1.34, m	1.36, m	1.33, m	1.32, m	1.32, m
3α	1.47, m	1.49, m	1.47, m	1.46, m	1.48, m
3β	1.16, m	1.18, m	1.15, m	1.16, m	1.16, m
5	1.45, d (7.0)	1.52, d (6.9)	1.43, d (7.2)	1.48, d (7.0)	1.59, d (6.9)
6	5.12, d (7.0)	5.14, d (6.9)	5.30, d (7.2)	5.13, d (7.0)	5.13, d (6.9)
9	2.00, m[a]	2.19, dd (11.1, 5.6)	2.41, dd (12.8, 5.6)	2.02, m[a]	2.13, m[a]
11α	1.46, m	1.48, m	1.52, m	1.44, m	1.41, m
11β	1.28, m	1.35, m	1.31, m	1.27, m	1.29, m
12α	2.18, m	2.05, m	2.26, m	1.85, m	2.03, m
12β	1.41, m	1.47, m	1.58, m	1.42, m	1.66, m
13	2.11, dd (10.4, 4.2)	1.74, dd (10.4, 4.0)	1.78, br d (10.6)	2.05, m[a]	1.95, dd (10.4, 4.0)
14α	1.79, d (12.5)	1.91, d (12.7)	4.79, br s	1.78, d (12.1)	1.76, d (13.0)
14β	2.18, dd (12.5, 4.2)	2.04, dd (12.7, 4.0)		2.07, m[a]	2.04, m[a]
15	5.16, s	5.29, s	5.67, s	5.04, s	4.71, s
17a	3.72, d (11.5)	2.75, d (4.4)	2.73, d (4.3)	3.65, d (10.3)	3.76, d (11.2)
17b	3.47, d (11.5)	2.69, d (4.4)	2.69, d (4.3)	3.56, d (10.3)	3.39, d (11.2)
18	0.80, s	0.82, s	0.81, s	0.80, s	0.83, s
19	1.09, s	1.10, s	1.14, s	1.09, s	1.09, s
20a	4.04, d (9.6)	4.08, d (9.6)	4.15, d (9.7)	4.04, d (9.5)	4.04, s
20b	3.84, d (9.6)	3.86, d (9.6)	3.83, d (9.7)	3.83, d (9.5)	3.84, s
AcO-6	2.01, s	2.00, s	1.97, s	2.00, s	2.01, s
AcO-15	2.18, s	2.16, s	2.16, s	2.17, s	2.25, s

[a]Signals were in overlapped regions of the spectra and the multiplicities could not be discerned.

Table 3. **^{1}H NMR Data for Compounds 6–10** ($CDCl_3$, 400 MHz, δ in ppm, J in Hz)

position	6	7	8	9	10
1α		1.44, m	1.40, m	1.97, m	
1β	4.72, dd (10.6, 5.2)	1.13, m	1.11, m	0.99, m	4.78, dd (10.1, 5.4)
2α	1.46, m	1.47, m	1.43, m	1.47, m	1.81, m
2β	1.75, m	1.32, m	1.27, m	1.52, m	1.49, m
3α	1.49, m	1.47, m	1.44, m	1.45, m	1.52, m
3β	1.30, m	1.17, m	1.14, m	1.25, m	1.47, m
5	1.37, d (6.7)	1.65, d (7.5)	1.34, d (5.6)	1.53, d (13.2)	1.51, m[a]
6	3.74, d (6.7)	5.18, d (7.5)	3.82, d (5.6)	5.53, d (13.2)	3.73, dd (11.5, 2.3)
					3.68, dd (11.5, 5.4)
9	2.50, dd (12.6, 5.8)	2.05, m[a]	1.96, dd (11.6, 6.0)	1.85, m[a]	2.50, m[a]
11α	1.60, m	1.45, m	1.42, m	1.68, m	1.31, m
11β	1.04, m	1.28, m	1.24, m	1.30, m	1.65, m
12α	2.35, m	2.19, m	2.16, m	1.86, m	1.82, m
12β	1.50, m	1.34, m	1.39, m	1.58, m	1.50, m
13	2.56, d (9.7)	2.60, dd (9.3, 4.6)	2.61, dd (8.5, 4.2)	2.79, dd (7.8, 3.8)	2.53, m[a]
14α	4.69, br s	1.81, d (12.3)	1.60, d (12.0)	2.10, m[a]	1.99, brd (12.4)
14β		1.68, dd (12.3, 4.6)	1.54, dd (12.0, 4.2)	1.60, m[a]	2.38, dd (12.4, 3.6)
15	6.05, s	5.64, br s	4.44, br s	6.14, t (2.5)	
16					2.51, m[a]
17a	5.16, br s	5.04, br s	5.07, br s	5.01, br s	1.17, d (6.9)
17b	5.07, br s	4.89, br s		4.99, br s	
18	1.02, s	0.84, s	0.99, s	1.06, s	1.05, s
19	1.11, s	1.10, s	1.06, s	0.96, s	0.86, s
20a	4.24, d (10.0)	4.08, d (9.6)	4.00, d (9.4)	1.31, s	4.87, d (12.1)
20b	4.15, d (10.0)	3.85, d (9.6)	3.86, d (9.4)		4.46, d (12.1)
AcO-1	1.99, s				2.03, s
AcO-6		2.06, s		2.15, s	
AcO-15	2.10, s	2.19, s		2.12, s	

[a]Signals were in overlapped regions of the spectra and the multiplicities could not be discerned.

Table 4. IC_{50} Values of Compounds 1–10 Inhibiting NO Production in BV-2 Cells

compound	IC_{50} (μM)[a]	compound	IC_{50} (μM)[a]
1	15.6	**7**	26.2
2	>100	**8**	>60
3	>100	**9**	7.3
4	44.1	**10**	>100
5	40.1	SMT[a]	3.6
6	>100		

[a]SMT(2-methyl-2-thiopseudourea, sulfate) was used as a positive control. Data are presented based on three parallel experiments.

Table 5. **Logarithms of Free Binding Energies (FBE, kcal/mol) of NO Inhibitors to the Active Cavities of iNOS (PDB code: 3E6T) and Targeting Residues of the Binding Site Located on the Mobile Flap**

compound	–log (FBE)	targeting residues			
1	–8.5	ARG-375	H4B-902	GLN-257	
4	–7.7	ARG-260	ARG-382	H4B-902	GLN-257
5	–8.1	ARG-260	ARG-375	ARG-382	TYR-367
7	–7.8	ARG-260	ARG-375	ARG-382	
9	–7.6	ARG-260	ARG-382		

Figure Captions

Figure 1. $^{1}H–^{1}H$ COSY and key HMBC correlations of compounds **1**–**10**.

Figure 2. Conformations and key NOESY correlations and of compounds **1**, **2**, **4**, **6**, **9**, and **10**.

Figure 3. Calculated and experimental ECD spectra for compounds **1**–**10** (A–J) in acetonitrile.

Figure 4. Molecular docking simulations obtained at lowest energy conformation, highlighting potential hydrogen contacts of compounds **1** (A), **4** (B), **5** (C), **7** (D), and **9** (E), respectively. (Color for atoms: cyan for carbon; blue for nitrogen; red for oxygen; gray for hydrogen; orange for sulfur). Only interacting residues are labeled for clarity. Hydrogen bonding interactions are shown by dashes. These figures were created by PyMOL.

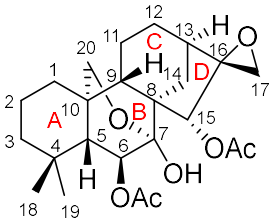

1

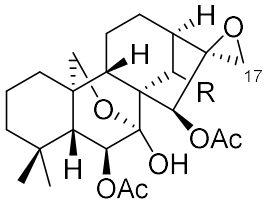

2 R = H
3 R = β-OH

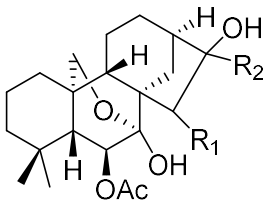

	R_1	R_2
4	α-OAc	β-CH_2OH
5	β-OAc	α-CH_2OH

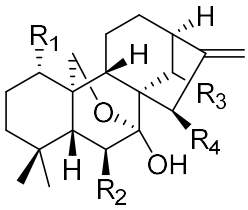

	R_1	R_2	R_3	R_4
6	OAc	OH	β-OH	OAc
7	H	OAc	H	OAc
8	H	OH	H	OH

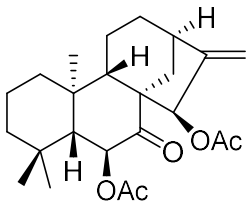

9

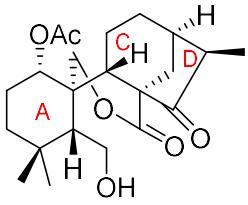

10

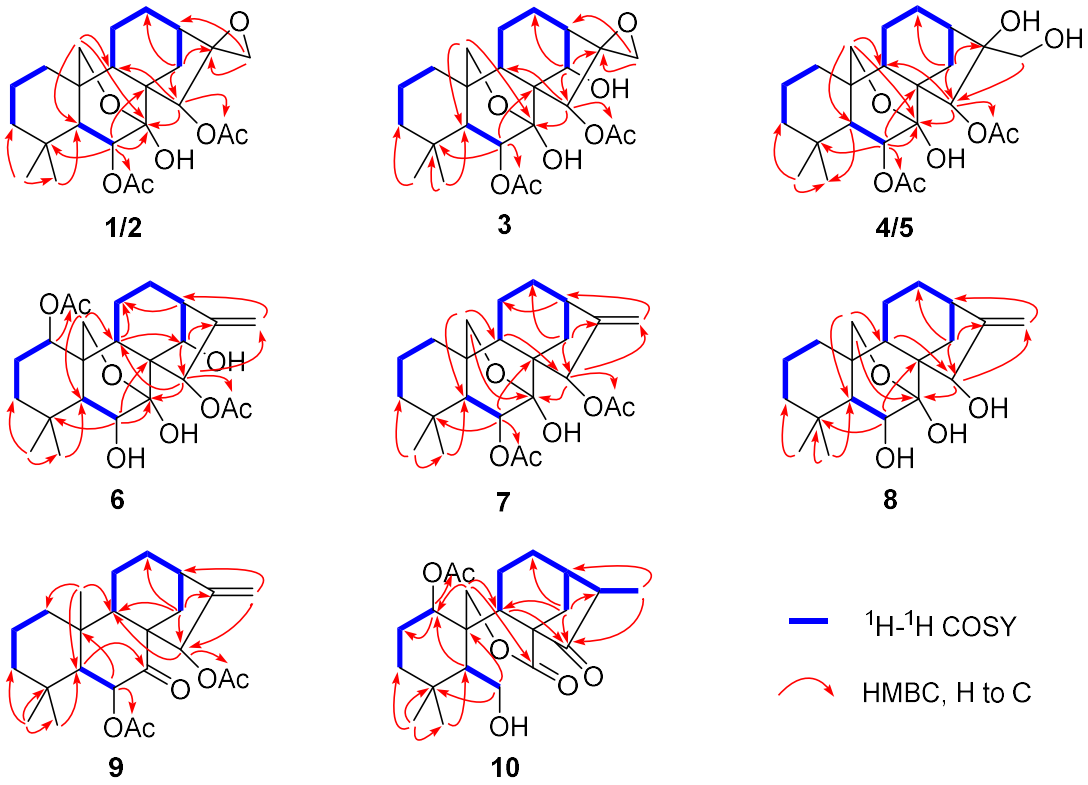

Figure 1. ^{1}H–^{1}H COSY and key HMBC correlations of compounds **1**–**10**.

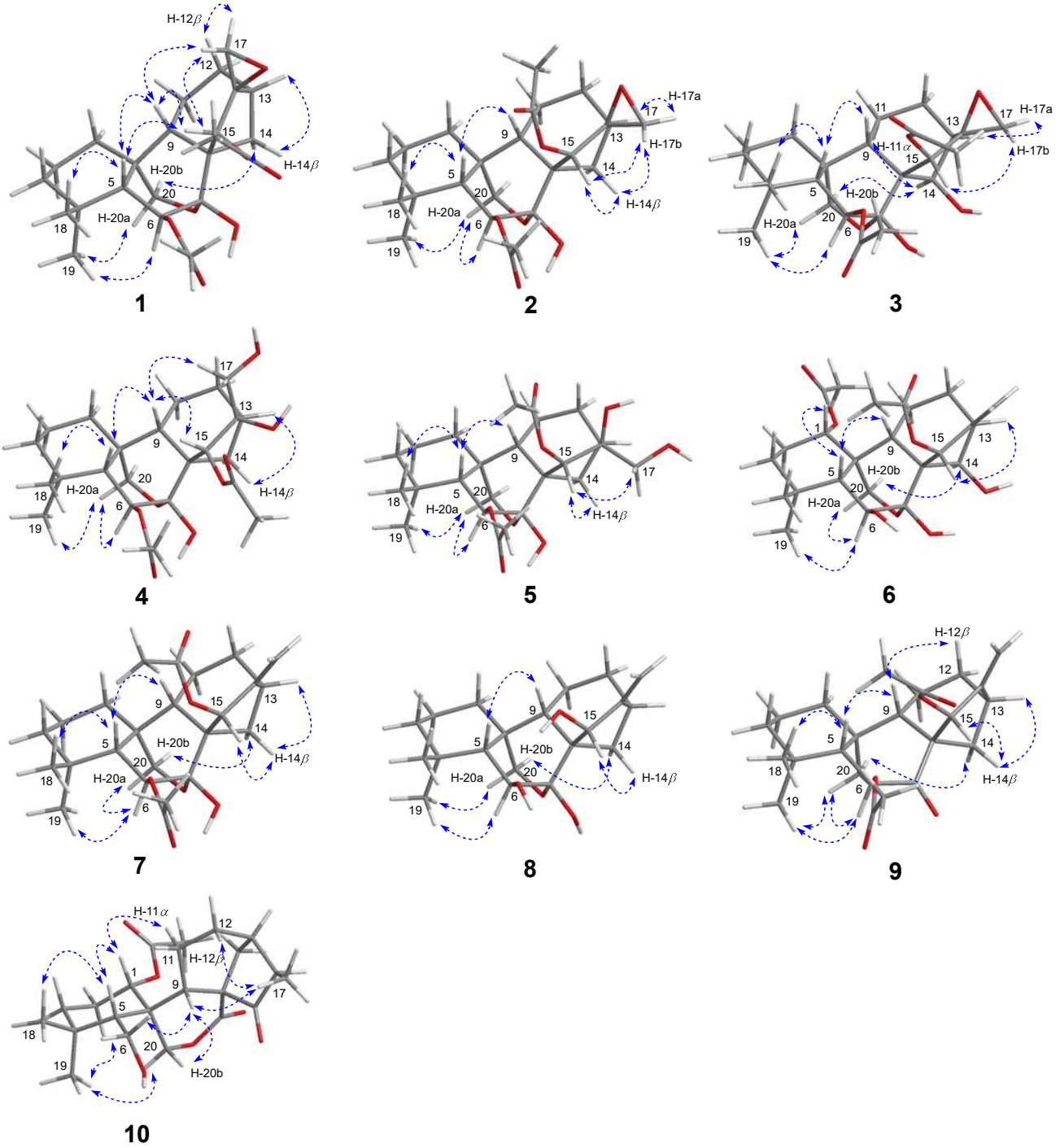

Figure 2. Conformations and key NOESY correlations and of compounds **1**–**10**.

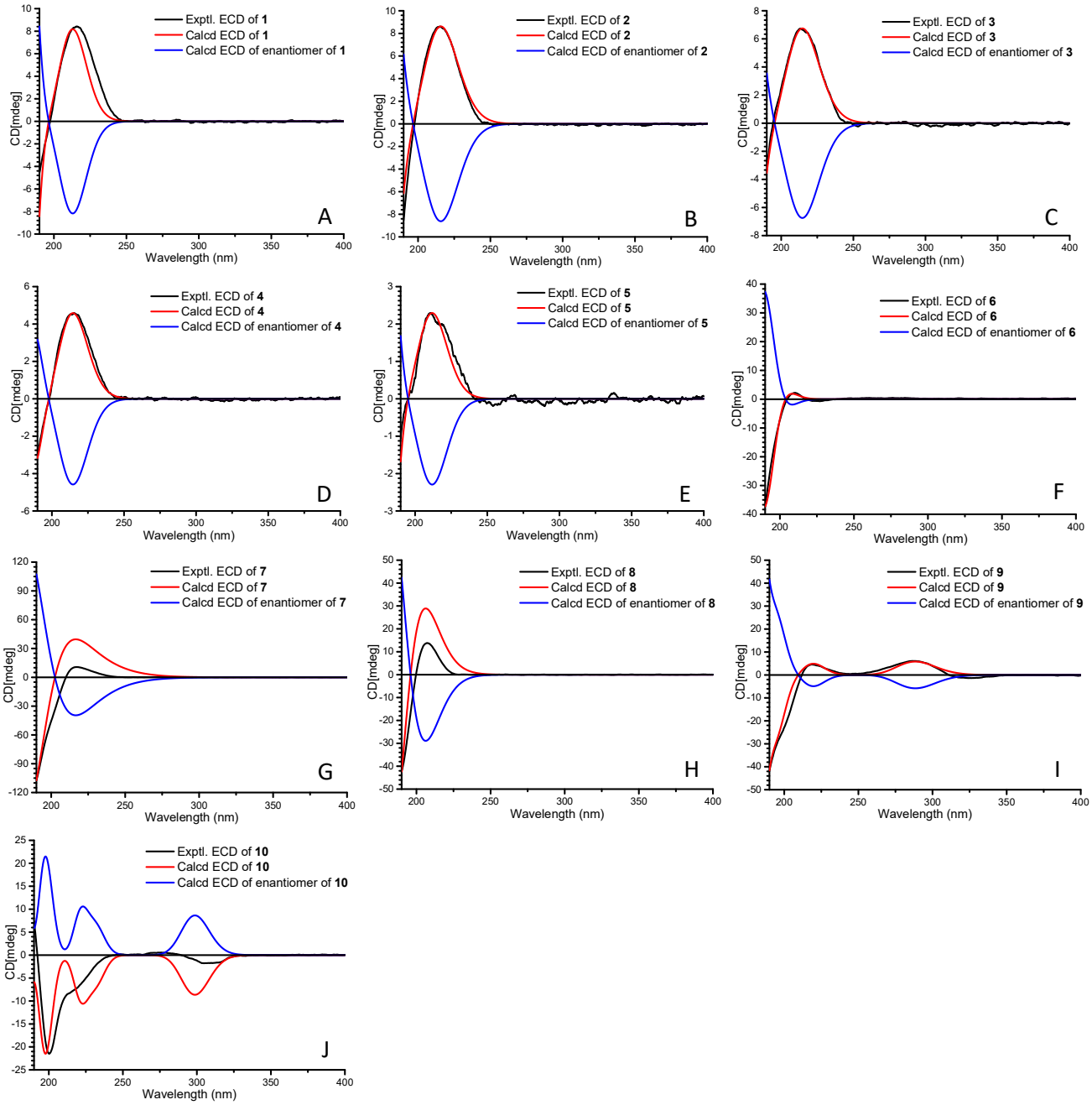

Figure 3. Calculated and experimental ECD spectra for compounds **1–10** (A–J) in acetonitrile.

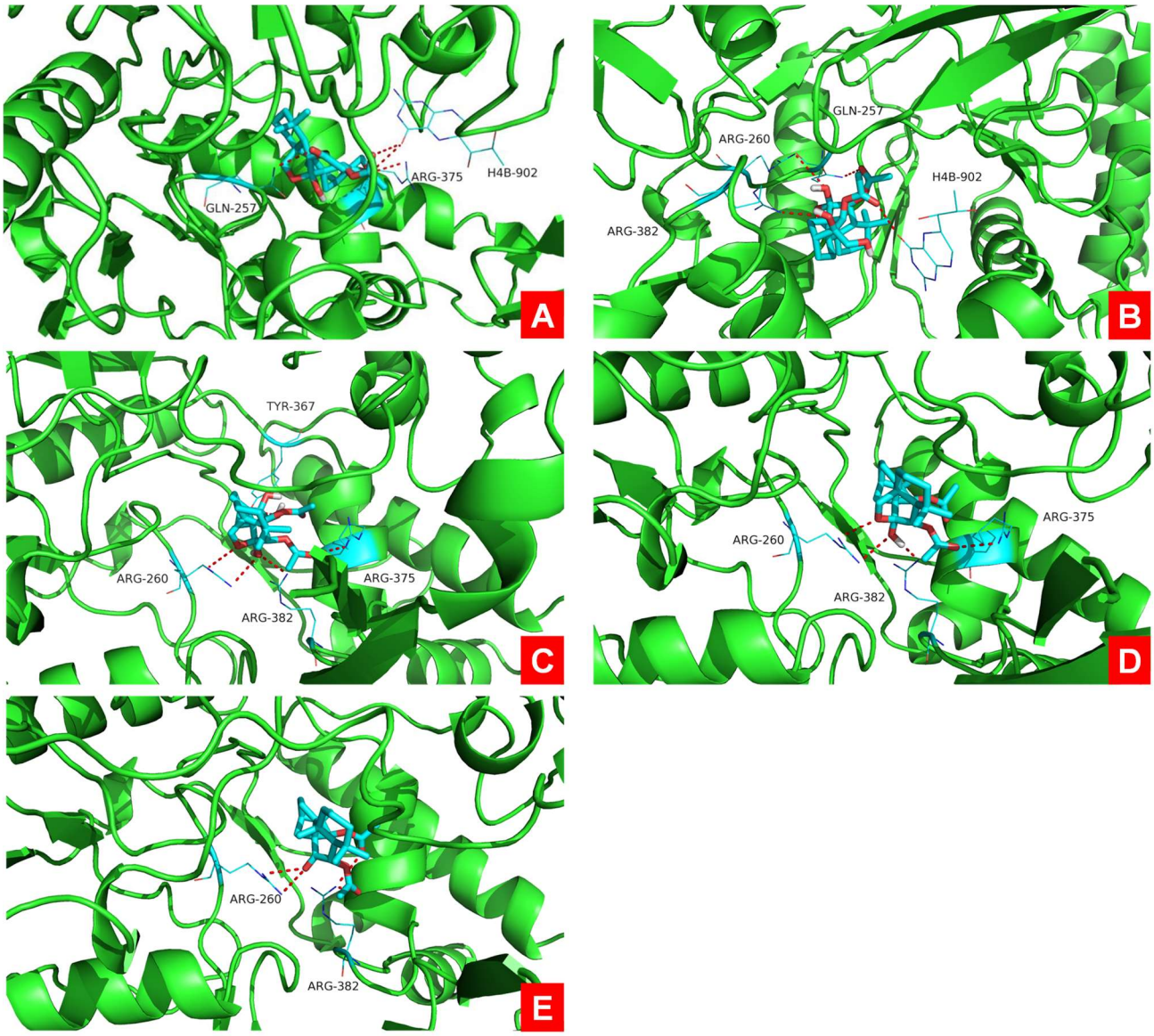

Figure 4. Molecular docking simulations obtained at lowest energy conformation, highlighting potential hydrogen contacts of compounds **1** (A), **4** (B), **5** (C), **7** (D), and **9** (E), respectively. (Color for atoms: cyan for carbon; blue for nitrogen; red for oxygen; gray for hydrogen; orange for sulfur). Only interacting residues are labeled for clarity. Hydrogen bonding interactions are shown by dashes. These figures were created by PyMOL.

Table of Contents/Abstract Graphic

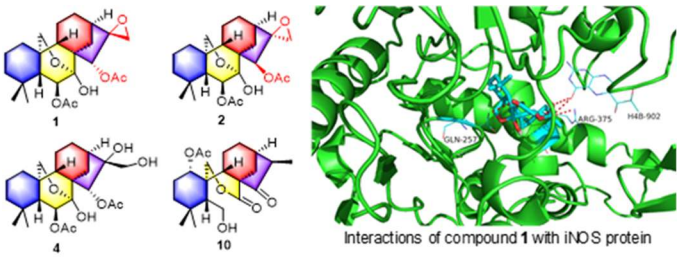

Interactions of compound **1** with iNOS protein